Chemical Science

ROYAL SOCIETY OF CHEMISTRY

EDGE ARTICLE

View Article Online
View Journal | View Issue

Cite this: *Chem. Sci.*, 2024, **15**, 7651

All publication charges for this article have been paid for by the Royal Society of Chemistry

Received 11th March 2024
Accepted 12th April 2024

DOI: 10.1039/d4sc01664e

rsc.li/chemical-science

Nanoelectrochemistry reveals how presynaptic neurons regulate vesicle release to sustain synaptic plasticity under repetitive stimuli†

Fu-Li Zhang,[a] Xiao-Ke Yang,[a] Yu-Ting Qi,[a] Si-Yu Tian[a] and Wei-Hua Huang *[ab]

Synaptic plasticity is the ability of synapses to modulate synaptic strength in response to dynamic changes within, as well as environmental changes. Although there is a considerable body of knowledge on protein expression and receptor migration in different categories of synaptic plasticity, the contribution and impact of presynaptic vesicle release and neurotransmitter levels towards plasticity remain largely unclear. Herein, nanoelectrochemistry using carbon fiber nanoelectrodes with excellent spatio-temporal resolution was applied for real-time monitoring of presynaptic vesicle release of dopamine inside single synapses of dopaminergic neurons, and exocytotic variations in quantity and kinetics under repetitive electrical stimuli. We found that the presynaptic terminal tends to maintain synaptic strength by rapidly recruiting vesicles, changing the dynamics of exocytosis, and maintaining sufficient neurotransmitter release in following stimuli. Except for small clear synaptic vesicles, dense core vesicles are involved in exocytosis to sustain the neurotransmitter level in later periods of repetitive stimuli. These data indicate that vesicles use a potential regulatory mechanism to establish short-term plasticity, and provide new directions for exploring the synaptic mechanisms in connection and plasticity.

Introduction

The nervous system, which is the integration and command center of mammals, regulates bodily functions such as learning, memory, motion, and emotion by precisely adjusting complicated neural networks. Communication between neurons relies on small synaptic vesicle (SV) exocytosis triggered by action potential (AP), and release of neurotransmitters such as dopamine (DA) that subsequently bind with postsynaptic receptors.[1,2] Synaptic plasticity represents the advanced regulatory capacity of neurons for synaptic strength while facing dynamic changes within, as well as environmental changes. This process is collectively modulated by synaptic protein expression, presynaptic vesicle release, and postsynaptic receptor migration.[3–6]

Among multiple forms of synaptic plasticity, short-term plasticity lasts from seconds to minutes and is mainly regulated by the amounts of neurotransmitters released from the presynaptic terminals.[4,7–9] Despite all the research that has been performed to elucidate the mystery of synaptic plasticity, the regulation of vesicular exocytosis and neurotransmitter release in different short-term plasticity categories remains ambiguous, due to a lack of analytical methods capable of quantitatively and kinetically measuring vesicular exocytosis inside synapses.[10]

Electrochemistry with micro- and nanoelectrodes has become a useful tool to monitor vesicular exocytosis and its quantitative and kinetic information at the single-cell level, and obtains results with high sensitivity and excellent spatio-temporal resolution.[11–16] By combining this method with intracellular vesicle impact electrochemical cytometry, which can quantify unreleased vesicular content,[17,18] the variability of exocytosis and the vesicular content of single pheochromocytoma PC12 cells under repetitive stimuli have been detected for the first time.[19–21]

These works successfully demonstrate exocytotic plasticity and its regulatory mechanisms at the single cell level. However, neurotransmitter release in synapses is regulated by a more complicated mechanism, and because of the small size of the synapse, it is extremely difficult to monitor vesicular exocytosis *in situ*. To realize measurement inside the synapse, conical carbon fiber nanoelectrodes (CFNEs) with a tip diameter as small as 50 nm have been developed for monitoring norepinephrine and DA exocytosis inside different synapses.[22–24] The inside-synapse measurement deepened our understanding of the exocytotic model and the dynamics of SVs, and subsequently prompted us to investigate quantitative and dynamic variations in SV exocytosis and the underlying regulatory mechanisms.

[a]*College of Chemistry and Molecular Sciences, Wuhan University, Wuhan 430072, P. R. China. E-mail: whhuang@whu.edu.cn*

[b]*Department of Hepatobiliary and Pancreatic Surgery, Zhongnan Hospital of Wuhan University, Wuhan 430071, P. R. China*

† Electronic supplementary information (ESI) available: Materials, experimental methods and supplementary figures and tables. See DOI: https://doi.org/10.1039/d4sc01664e

Herein, CFNE-based nanoelectrochemistry was adopted for real-time monitoring of DA release inside single dopaminergic (DAergic) synapses, as well as the plasticity variations of these synapses under repetitive electric field stimulus (EFS), as shown in Fig. 1. We found that despite different details obtained based on cell heterogeneity, presynaptic neurons maintained neurotransmitter release by rapidly recruiting SVs and changing exocytotic dynamics, accompanied by the release of dense core vesicles (DCVs) at the late stage of stimuli. These data indicate a potential presynaptic regulatory mechanism to establish short-term plasticity, and provide a new angle to explore the mystery of synaptic connection and synaptic plasticity.

Results

Real-time measurement of DA exocytosis inside synapses under EFS

Synaptic plasticity is collectively modulated by presynaptic and postsynaptic mechanisms. To focus on presynaptic exocytosis while avoiding postsynaptic effects, DAergic neurons were selected (identified by fluorescent imaging, as shown in Fig. S1†) that contain metabotropic DA receptors that do not retrogradely regulate presynaptic exocytosis in a short time.[25] Cone-shaped CFNEs with a tip diameter of 50 nm and length of approximately 1 μm with excellent electrochemical performance and quantitative capability of DA (Fig. S2†) were fabricated to match the nano-size synaptic cleft. The entire conical CFNE nanotip was able to penetrate into the synapse and be tightly sealed. This process was confirmed by the progressive decrease (as the insertion depth increased) of $Ru(NH_3)_6^{3+}$ voltammetric current intensity in a cell bath (Fig. S3†). After withdrawal of the CFNE from the synapse, the voltammetric current was completely restored. This ensured that the signals obtained during the following electrochemical measurements were derived from presynaptic vesicle release, and the insertion process did not affect the sensitivity of the CFNEs.

Because the residual K^+ surrounding the neurons may result in multiple AP after a single stimulus when a high K^+ solution was applied to evoke vesicular exocytosis, we chose EFS to evoke a single nervous impulse and distinguish the effects of each single AP.[26,27] As the fluorescent tests show in Fig. S4 and S5,† AP was successfully triggered by EFS, as evidenced by the increase in the intracellular Ca^{2+} concentration. Numerous amperometric spikes were detected when a DAergic synapse activated by EFS was probed by a CFNE (Fig. S6A†), while no spikes were detected without EFS or extracellular calcium (Fig. S7†). This demonstrated that these spikes correspond to sequential vesicular release from single SVs.

We succeeded in detecting a small number of synchronous exocytotic events (spikes occurring within 200 ms after EFS) and a mass of asynchronous exocytotic events (spikes occurring during a later period), which was in agreement with the exocytosis model of periglomerular neurons and adrenal chromaffin cells,[28,29] and all these events were considered in the following analysis. According to the shape and kinetic parameters of single exocytotic events, these spikes can be divided into two modes: simple spikes with a rising phase followed by a single falling phase (spike a, shown in Fig. S6†) and complex spikes exhibiting multiple sub-spikes or a plateau shape with longer duration (spike b and spike c in Fig. S6†).

Statistical analyses of the recorded individual amperometric spikes (complex spikes were excluded) allowed us to obtain quantitative and kinetic information for SV exocytosis. As shown in Fig. S6B and S8,† the time width at half maximum ($t_{1/2}$), individual peak currents (I_{max}), and peak area (Q, being proportional to the number N of released DA molecules according to Faraday's law, $N = Q/2F$, where $F = 96\,500$ C mol^{-1} is the Faraday constant) are 0.19 ± 0.03 ms, 17.9 ± 4.7 pA, and 12 700 ± 3300 molecules (mean ± SEM, $n = 494$), respectively.

Then, the SV release under repetitive EFS was measured. The interval of periodic EFS was set as 70 s to ensure the recovery of the active zone and vesicular loading.[27] Each synapse underwent stimulation at least 10 times, and the measurement terminated when there was no current spike in two continuous stimuli. Four representative amperometric traces recorded under different stimulus times are shown in Fig. 2A.

Fig. 2B provides quantitative information regarding the exocytotic event number (frequency of the exocytotic events, F_{event}) and the total amount of released molecules (the sum of N of each spike, N_{total}) from the same synapse under each stimulus. Simple and complex spikes are included in this analysis. We discovered the same tendency in multiple neurons, whereby stimuli times increased, and both F_{event} and N_{total} then underwent an early decrease and late recovery. For example, in Fig. 2B, F_{event} and N_{total} continued to decrease after the initial 5 stimuli, then visibly increased at the 6th stimulus, reached a peak value at the 13th stimulus, and then ultimately decreased to no occurrence of exocytosis.

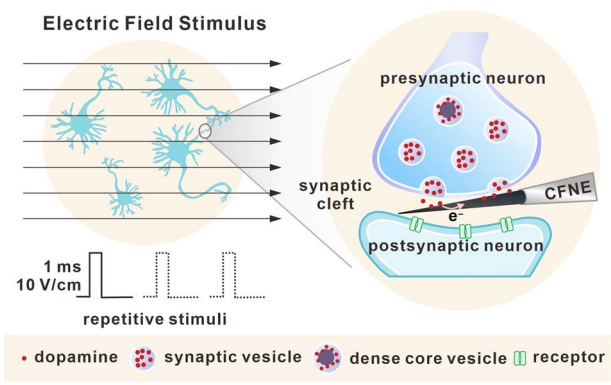

Fig. 1 Schematic of electric field stimulus and repetitive stimuli towards DAergic neurons, as well as amperometric detection of exocytosis inside a single synaptic cleft.

The presynapse maintains a releasable vesicle amount under repetitive stimuli

Exocytotic events in additional synapses under repetitive EFS were amperometrically measured to further investigate the variations of exocytosis. The statistics for two important parameters, F_{event} and N_{total}, from 5 representative synapses are summarized in Fig. 3A. For each synapse, the results under four representative stimuli (first one, the stimulus with minimum F_{event} before recovery, the stimulus with maximum F_{event} during recovery, and the last one

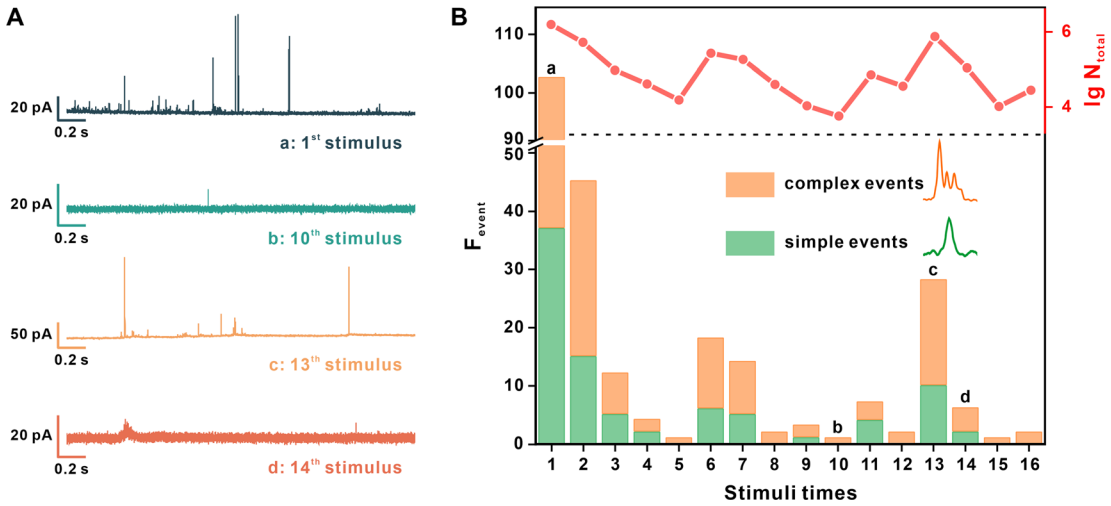

Fig. 2 The variation of neuronal exocytosis under repetitive stimuli. (A) Four representative amperometric traces recorded by a CFNE from the same DAergic synapse after different stimuli times. (B) Frequency histograms describing the simple and complex event amount (F_{event}) after each EFS, and line graphs describing the total number of released DA molecules (N_{total}) during each stimulus, quantified from amperometric traces of the same synapse shown in (A).

with detected exocytotic events) were chosen for analysis. Because of cell heterogeneity, the stimulus numbers corresponding to the above four stages were different between synapses.

By comparing the data for different stimuli times with that for the first stimulus (Fig. 3A), we found that F_{event} and N_{total} underwent an early decrease and late increase with different degrees of recovery, with partial recovery in synapse 1–2, full recovery in synapse 3, and potentiation of synaptic strength in synapse 4–5. Therefore, we concluded that in the initial stage of repetitive EFS, the vesicles in the readily releasable pool (RRP) were gradually consumed, manifesting as continuously decreased exocytotic events. To maintain the vesicular amount in the RRP and fundamental synaptic transmission, presynaptic neurons might aggregate additional vesicles by expediting the vesicular cycle or recruiting additional vesicles from the cell body, which contributes to the recovery of F_{event} and N_{total} for signal transmission in the synapse under repetitive stimuli.

Despite different neurons showing different timing nodes at which the above changes of F_{event} and N_{total} occurred under repetitive EFS, the F_{event} and N_{total} of most synapses exhibited recovery after the 10th stimulus. Hence, we uniformly selected and compared the 1st and 10th stimuli to explore the vesicular supplemental mechanism under repetitive EFS.

Exocytosis arises by presynaptic Ca^{2+} influx, and Ca^{2+} is a ubiquitous second messenger that plays important roles in a variety of physiologic events. We first investigated the variation in intracellular Ca^{2+} concentration. In Fig. 3B, fluorescence statistical analysis revealed that reduplicative EFS led to an increase in the intracellular Ca^{2+} concentration. Ca^{2+} accumulation may activate calmodulin and Ca^{2+}/calmodulin-dependent protein kinase II (CaMKII) for vesicular assembly and contribute to the recovery of the releasable vesicle amount and maintenance of synaptic strength under repetitive stimuli.[4,30]

Synaptophysin, a glycoprotein located on SVs,[31,32] was immunofluorescently stained to examine any changes in vesicular density. To be consistent with the above results (*i.e.*, the vesicular exocytosis and Ca^{2+} imaging after the 1st and 10th stimuli), the vesicular distribution before the 1st (without stimulus) and 10th stimulus (after the 9th EFS) were quantified. As shown in Fig. 3C and D, the vesicular density obviously increased after the 9th stimulus. We also used transmission electron microscopy (TEM) to count the number of vesicles in the ventral tegmental area (VTA) presynaptic terminal from brain slices that underwent identical stimuli (Fig. 3E).

Fig. 3F shows that the vesicle number in the active zone, defined as the area within a 200 nm distance from the presynaptic membrane,[33] maintained the same level after iterative stimuli. The total number of vesicles increased to 51 ± 11 after 9 stimuli, in comparison with 34 ± 12 in neurons without stimulus (Fig. 3G). These results from cultured neurons and brain slices suggested that a rapid vesicular complementary mechanism involving vesicular formation and recruitment is invoked in synaptic plasticity under repetitive EFS, and this replenishment mechanism might be related to increased intracellular Ca^{2+} concentration.

Synaptic vesicles tend to release a greater fraction of content by adjusting dynamics under repetitive stimuli

Synaptic plasticity can also be regulated by exocytosis mode, which is reflected by the vesicular release fraction or dynamics.[11,22,23] For easier comparison and elimination of the effects of cell heterogeneity, we equally divided all the amperometric traces recorded in a synapse into two groups (former half stimuli and latter half stimuli on the basis of stimuli times), and compared the average number of released molecules ($\bar{N}$) and the kinetic parameters between the two groups (Fig. 4A–C).

$\bar{N}_{former}$ and $\bar{N}_{latter}$ represent the average number of released molecules for all events detected under former and latter half stimuli, respectively. The results showed that $\bar{N}_{latter}$ was obviously larger than $\bar{N}_{former}$ (Fig. 4A), suggesting that SVs tend to add neurotransmitter release after repetitive EFS. Two kinetic

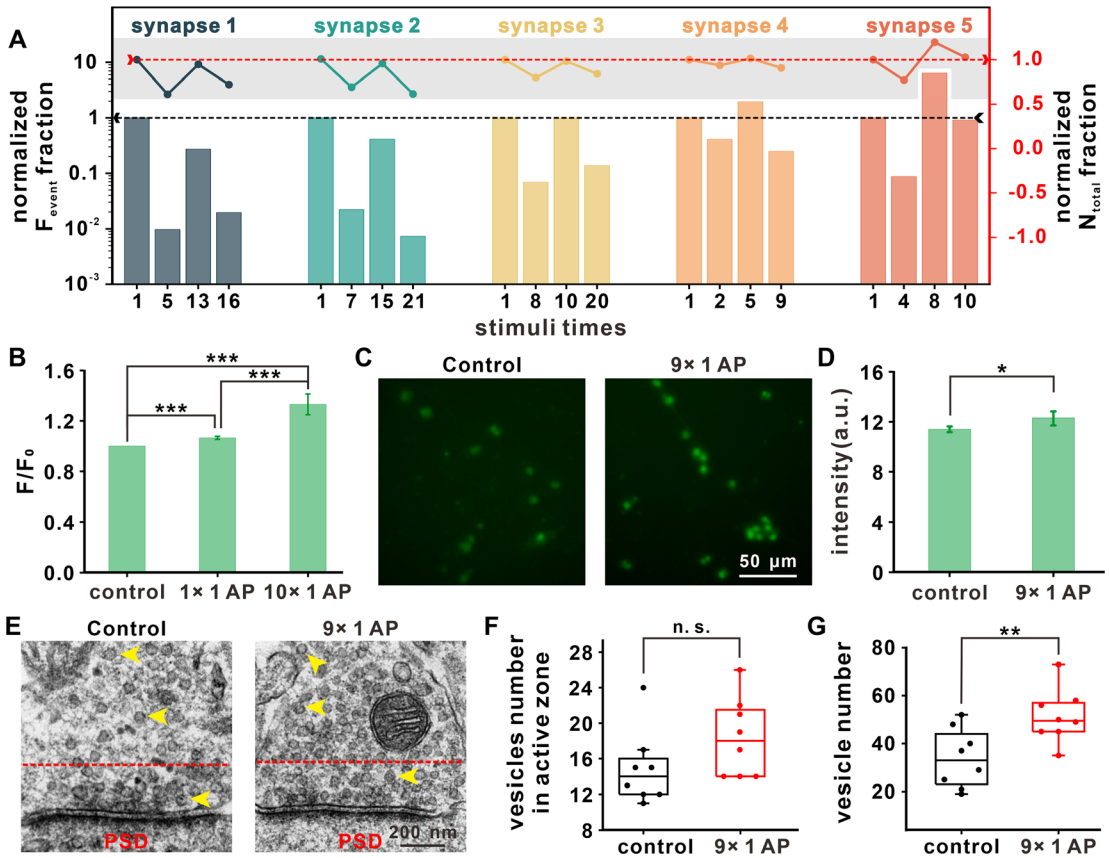

Fig. 3 The variation in the neuronal vesicle amount after repetitive stimuli. (A) Normalized histograms of F_{event} under representative stimuli times (first one, the stimulus with minimum F_{event} before recovery, the stimulus with maximum F_{event} during recovery, and the last one with detected exocytotic events) compared with the event amount of the same synapse ($n = 5$) in the first stimulus, and normalized line graphs of N_{total} under different stimuli times compared with the release number of the same synapse in the first stimulus. (B) Normalized fluorescence statistical analysis of the same DAergic neuron ($n = 72$) showing the change in the intracellular Ca^{2+} concentration revealed by Fluo-4 AM before or after the first and 10th EFS; mean ± SD, ***$p \leq 0.001$. (C) Representative microscopic images of DAergic neurons without EFS or with 9 stimuli labeled with synaptophysin (SV marker, green), and the (D) corresponding statistical analysis; mean ± SD, *$p \leq 0.05$. (E) TEM images of SVs (marked by yellow arrows) in the VTA presynaptic terminal from 7 days SD rat brain slices without EFS or with 9 stimuli (PSD: post synaptic density), and the corresponding statistical analysis of the vesicle number in the active zone (the area between the red dashed line and the presynaptic membrane), which is defined as the area within a 200 nm distance from the presynaptic membrane (F), and in the (G) total presynaptic structure; $n_{cell} = 8$ in each group, n.s.: no significance, **$p \leq 0.01$.

parameters for simple exocytotic events, I_{max} (depending on the size of the fusion pore and the DA concentration inside the vesicle) and $t_{1/2}$ (representing the duration of the exocytotic event), were analyzed, where $\bar{I}_{max}$ and $\bar{t}_{1/2}$ denote the average value of all simple events in each synapse. As shown in Fig. 4B and C, $\bar{t}_{1/2}$ and $\bar{I}_{max}$ of latter half stimuli were larger than that of former half stimuli in most synapses. Because there was no significant change in vesicular size under repeated stimuli (Fig. S9†), I_{max} may be impacted by the enlargement of fusion pores, exhibiting the tendency of the synapse to expand the fusion pore. Prolonged $\bar{t}_{1/2}$ showed that the fusion pore duration may be extended. These dynamic changes occur to release more neurotransmitters for sustaining synaptic transmission after a mass of vesicular consumption.

Actin is a protein widespread in presynaptic that dynamically polymerizes and forms filamentous actin, which can prevent SVs from engaging in premature non-regulated fusion.[34] The disassembly of actin, triggered by a Ca^{2+} influx, is involved in vesicle exocytosis and modulates its dynamics. Hence, further detection of actin by immunofluorescence, as shown in Fig. 4D and E, proves that repetitive EFS facilitates actin disassembly, which might enlarge and stabilize fusion pores, as revealed by the amperometric record, and ultimately lead to more vesicular content release and a higher release fraction to maintain the synaptic transmission (Fig. 4F).

DCV release is involved in regulating synaptic plasticity under repetitive EFS

When comparing the $t_{1/2}$ of simple amperometric spikes, we found that except for standard simple spikes with an average $t_{1/2}$ of approximately 0.2 ms (Fig. 5A), there were long-duration simple events in the later period of repetitive EFS, although the frequency was very low (approximately 0.5% occurrences in all detected events). As shown in Fig. 5B and Table S1,† the $t_{1/2}$ values for these long-duration simple spikes (0.6–3 ms) were between the $t_{1/2}$ values of typical large DCVs (LDCVs, approximately 10 ms in Fig. S10†) from rat adrenal chromaffin cells and those of SVs (with a maximum of approximately 0.5 ms, as

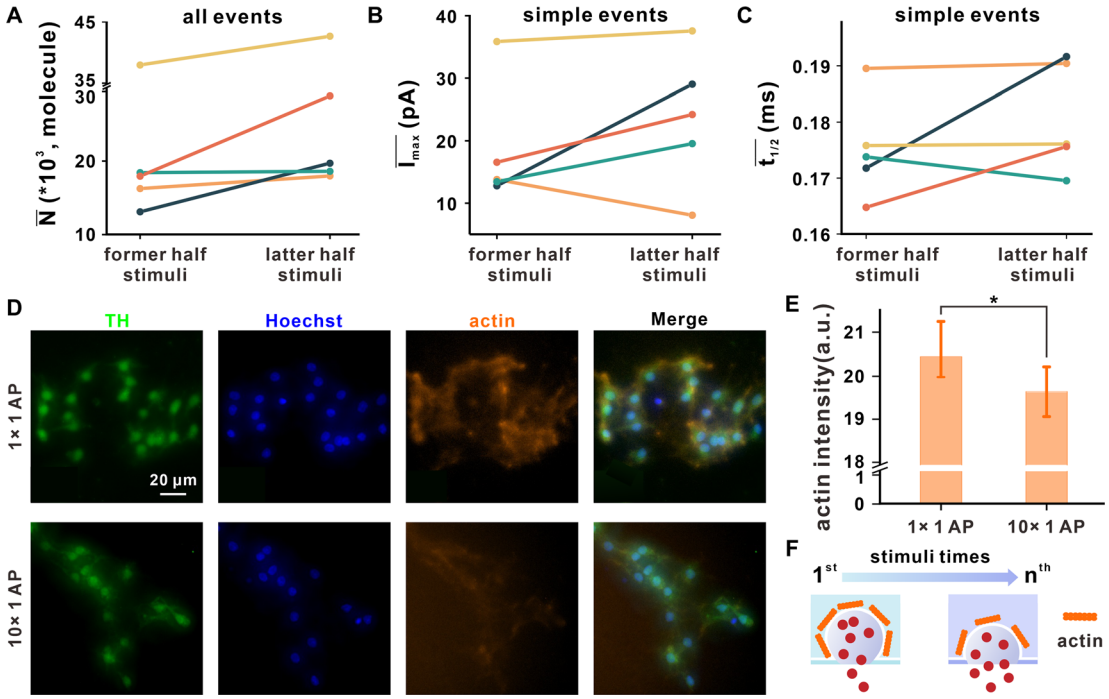

Fig. 4 The variation in neuronal vesicle exocytosis dynamics after repetitive stimuli. The (A) $\bar{N}$ of all events, (B) $\bar{I}_{max}$, and (C) $\bar{t}_{1/2}$ of simple events in former and latter half stimuli, while the entire repetitive stimuli process was equally divided into two groups according to stimuli times, and the different colors represent the data from different synapses corresponding to Fig. 3A. (D) Representative microscopic images of DAergic neurons after EFS for 1 time or 10 times, co-labeled with TH (DAergic neuronal marker, green), Hoechst stain (cell nucleus marker, blue) or phalloidin (actin marker, orange). (E) Corresponding statistical analysis of the average phalloidin fluorescence intensity of a single cell per image; $n_{1\times1AP} = 14$, $n_{10\times1AP} = 11$, mean ± SD, *$p \leq 0.05$. (F) Scheme proposed for the possible effect on vesicle exocytosis dynamics under repetitive stimuli with disassembly of actin.

shown in Fig. S8†), and displayed different exocytosis dynamics with these two types of traditional spikes. Therefore, we considered whether these long-duration simple spikes were generated by the exocytosis of DCVs in the presynaptic terminal.

These medium-sized DCVs (100 nm diameter) are common in the central nervous system, containing both neurotransmitters and neuromodulators (such as neuropeptides and hormones), and accounting for a very small percentage in presynaptic structure.[35,36] Although DCVs with large neurotransmitter content and neuromodulators are thought to be involved in adjusting synaptic activity, no direct observation of DCVs have been found. In this work, we attributed long-duration simple spikes to DCV release, because the exocytosis dynamics of long-duration simple spikes are in agreement with vesicle release with a dense core. In the case of single vesicle exocytosis, DCVs released a much greater number of neurotransmitters as compared to that of SVs (Fig. 5C). TEM images of brain slices also showed the existence of DCVs in the VTA presynaptic terminal. In Fig. 5D, DCVs possessing a dense core and halo (between the dense core and vesicular membrane) were found in synapses without EFS or those that underwent 9 stimuli. However, DCV release featured as simple spikes with much longer duration can only be observed in the late period of repetitive stimuli. These results showed that DCV release may be involved in short-term synaptic plasticity and significantly contribute to maintaining a moderate synaptic transmission level, especially when SVs are gradually consumed in the late period of repetitive stimuli.

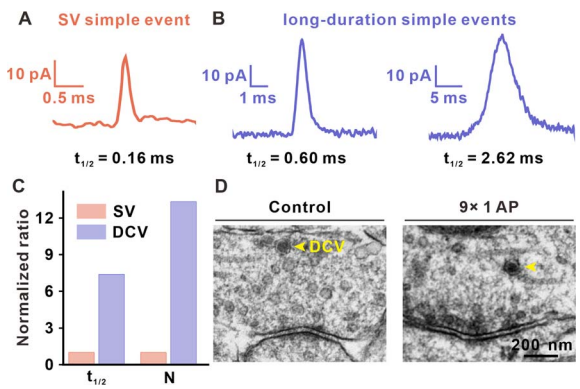

Fig. 5 DCV release after repetitive stimuli. (A) Typical spike of a simple SV exocytosis event from a DAergic neuron. (B) Typical spikes of long-duration simple events after repetitive stimuli. (C) Normalized comparison of $t_{1/2}$ and N in simple DCV-like events with simple SV events. (D) TEM images of SVs and DCVs (marked by yellow arrows) in a VTA synapse from 7 days Sprague-Dawley (SD) rat brain slices without EFS or with stimuli of 9 times.

Discussion

Synaptic plasticity is essential for the maintenance of various neural functions, especially for learning and memory. Presynaptic and postsynaptic mechanisms co-contribute to the expression of synaptic plasticity. Although the effect of

postsynaptic structure has been well studied mainly by electrophysiology,[5,8] less of a breakthrough has been achieved in unraveling the presynaptic contribution to synaptic plasticity, due to a lack of analytical methods able to detect vesicular exocytosis and its change inside the synapse. In this work, nanoelectrochemistry using CFNEs with excellent spatio-temporal resolution was applied for the real-time detection of presynaptic vesicle release of DA and its variations in quantity and kinetics under repetitive electrical stimulus (Fig. 6). We found that repetitive EFS rapidly consumed the readily releasable SVs in the presynaptic terminal as F_{event} and N_{total} obviously decreased (Fig. 2). To maintain synaptic strength, the presynaptic terminal tended to promptly recruit SVs (Fig. 3) and modulate the dynamics of SV exocytosis (Fig. 4) by enlarging the size of fusion pores and extending the duration of single exocytotic events to maintain sufficient neurotransmitter release following stimuli. Except for SVs, DCVs are involved in exocytosis to sustain neurotransmitter levels inside synapses during later periods of repetitive stimuli (Fig. 5).

Vesicles and exocytosis are important determinants of synaptic efficacy and plasticity. When neurons are evoked by AP, vesicles in the presynaptic RRP are rapidly consumed after being triggered by high local but short-life Ca^{2+} concentration. In the early stage of repetitive stimuli, the slow replenishment speed of readily released vesicles causes a depression in synaptic plasticity as the exocytosis event number and DA release decreases (Fig. 2). After the termination of nerve impulses, Ca^{2+} channels close, and the spatial gradient of Ca^{2+} concentration instantly collapses as Ca^{2+} diffuses and binds with calcium-binding proteins. Whereas, residual Ca^{2+} at a low concentration and long lifetime plays an important role in activity-dependent short-term plasticity.[4,8,30,37]

As stimuli times increase, residual Ca^{2+} accumulates, causing an increase in Ca^{2+} concentration in the presynaptic terminal (Fig. 3B), which leads to vesicular aggregation in the presynaptic bouton (Fig. 3G). The generation speed of newborn vesicles accelerates as the vesicular density increases after repeating stimuli (Fig. 3C and D). This might result from residual Ca^{2+} and CaMKII-activated phosphorylation of cAMP-responsive element binding protein (CREB), a cellular transcription factor for altering the transcription of the downstream genes relevant to vesicular cycle and exocytosis.[9]

The rapid vesicular aggregation and generation guarantee the maintenance of the vesicular amount in active zones and recovery of the exocytotic event amount after repetitive stimuli (Fig. 2). As for different degrees of recovery, they are mainly attributed to the primary release possibility of the different synapses. The synapses (such as synapse 1 and synapse 2 in Fig. 3) with more readily releasable vesicles underwent greater vesicular consumption during repetitive stimuli, hence showing a high degree of depression before recovery and partial recovery in the latter period.

Exocytosis dynamics can be modulated to change the amount of released neurotransmitter and the synaptic strength. We analyzed I_{max} and $t_{1/2}$ for simple events, which represent the size of the fusion pore and duration of exocytosis, respectively, to explore the change in exocytotic dynamics during activity-dependent short-term plasticity. In the static state, vesicles are retained in a highly dense actin network. Upon nerve impulse, the actin network was disassembled by Ca^{2+}-activated actin-severing proteins such as gelsolin, and vesicles decomposed the actin network for further exocytosis.[38]

Actin disassembly is highly involved in exocytosis dynamics by regulating the opening and closing of fusion pores. During repeating EFS, the accumulation of residual Ca^{2+} leads to a high degree of actin disassembly (Fig. 4D and E), which results in enlargement of fusion pores and prolongation of simple spike duration, and is shown as an increase in I_{max} and $t_{1/2}$ in amperometric signals. Hence, the presynaptic terminal tends to release a greater fraction of DA for maintenance of synaptic transmissions.

Most synapses and axons in the central nervous system contain few DCVs participating in synaptic transmission and regulation.[39–41] However, because of the similarity with SVs and the rarity of DCVs, it is difficult to monitor and explore the effects of DCVs, especially inside the synapse. DCVs possess a dense core and store abundant neurotransmitters in the halo and the dense core. For hindrance of the dense core, it is necessary for DA to diffuse along the halo until it arrives at the fusion pore, and a long displacement distance increases exocytosis duration. And some DA binds with the dense core matrix and requires time for DA-matrix unbinding, which also increases the duration of exocytosis. Therefore, we successfully distinguished and classified each single exocytotic event from SVs or DCVs by analyzing the amperometric spike parameters I_{max} and $t_{1/2}$.

The Ca^{2+}-dependent activator protein for secretion (CAPS) is a protein related to DCV release, with a low affinity for binding with Ca^{2+}.[30,42] Consequently, DCV release requires a greater increase in the synaptic Ca^{2+} concentration until CAPS is activated by sufficient surrounding Ca^{2+},[36] which is satisfied by residual Ca^{2+} aggregation under enhanced stimuli. For this reason, we succeeded in monitoring a small amount of DCV secretion in the later stage of repeating stimuli (Fig. 5 and Table

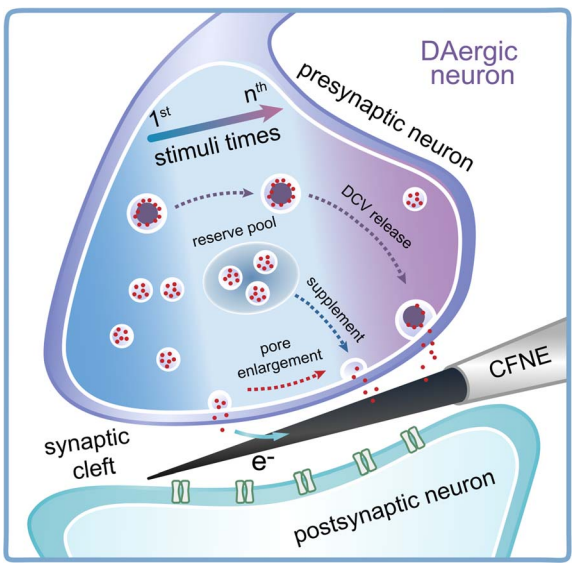

Fig. 6 Schematic showing the change in vesicle recycling and exocytosis dynamics accompanying DCV release inside DAergic synapses under repetitive stimuli.

S1†), in accord with the rarity and slow replenishment speed of DCVs in the presynaptic bouton. The same measurements were also performed on single isolated varicosities (without post-synaptic connection), but no DCV release was found. This indicates that the involvement of DCVs is possibly a unique characteristic in synaptic modulation and plasticity.

Conclusions

In summary, we used a nanoelectrode to probe inside a single synapse of DAergic neurons and quantitatively monitored vesicular release under repetitive electrical stimuli to explore the presynaptic effect in synaptic plasticity. We found that early decrease and late recovery of presynaptic exocytosis occurs under repeating stimuli. During recovery, the presynaptic terminal tended to increase the exocytotic frequency by rapidly recruiting vesicles and releasing more DA by changing the exocytosis dynamics, along with DCV release (Fig. 6). The detection of synaptic exocytosis provides straightforward evidence of presynaptic participation and specific modulation of exocytosis in activity-dependent short-term plasticity. This work emphasizes the importance of presynaptic plasticity in the nervous system and offers new strategies and directions for investigating synaptic plasticity and the mechanisms governing learning and memory.

Ethical statement

The animal experimental protocols used in this study were approved by the Center for Animal Experiments of Wuhan University (SCXK(E)2019-0004). The experiments also comply with the 'Animal Research: Reporting *In Vivo* Experiments' (ARRIVE) 2.0 guidelines (**https://arriveguidelines.org/arrive-guidelines**).

Data availability

All experimental and characterization data and detailed experimental procedures are available in the published article and the ESI.†

Author contributions

W. H. and F. Z. designed the research. F. Z. performed the research. X. Y. and F. Z. analyzed the data. Y. Q. and S. T. provided technical support and suggestions. W. H. and F. Z. wrote the paper. All authors discussed the results and commented on the manuscript.

Conflicts of interest

There are no conflicts to declare.

Acknowledgements

The authors gratefully acknowledge the financial support from the National Natural Science Foundation of China (Grants 21725504, 22090050, 22090051, and 21721005) and the China Postdoctoral Science Foundation (Grants 2022M722456).

References

1 R. Jahn and D. Fasshauer, *Nature*, 2012, **490**, 201–207.
2 T. C. Südhof, *Neuron*, 2013, **80**, 675–690.
3 H. W. Tao and M. Poo, *Proc. Natl. Acad. Sci. U. S. A.*, 2001, **98**, 11009–11015.
4 R. S. Zucker and W. G. Regehr, *Annu. Rev. Physiol.*, 2002, **64**, 355–405.
5 R. A. Nicoll, *Neuron*, 2017, **93**, 281–290.
6 Y. Park, D. Jun, E. Hur, S. Lee, B. Suh and K. Kim, *J. Endocrinol.*, 2006, **147**, 1349–1356.
7 D. Fioravante and W. G. Regehr, *Curr. Opin. Neurobiol.*, 2011, **21**, 269–274.
8 W. G. Regehr, *Cold Spring Harbor Perspect. Biol.*, 2012, **4**, a5702.
9 R. Fukaya, H. Hirai, H. Sakamoto, Y. Hashimotodani, K. Hirose and T. Sakaba, *Sci. Adv.*, 2023, **9**, eadd3616.
10 J. A. Frank, M. Antonini and P. Anikeeva, *Nat. Biotechnol.*, 2019, **37**, 1013–1023.
11 E. V. Mosharov and D. Sulzer, *Nat. Methods*, 2005, **2**, 651–658.
12 R. M. Wightman, *Science*, 2006, **311**, 1570–1574.
13 N. T. N. Phan, X. Li and A. G. Ewing, *Nat. Rev. Chem*, 2017, **1**, 48.
14 J. Li, Z. Peng and E. Wang, *J. Am. Chem. Soc.*, 2018, **140**, 10629–10638.
15 K. Hu, Y. L. Liu, A. Oleinick, M. V. Mirkin, W. H. Huang and C. Amatore, *Curr. Opin. Electrochem.*, 2020, **22**, 44–50.
16 A. Shekar, S. J. Mabry, M. H. Cheng, J. I. Aguilar, S. Patel, D. Zanella, D. P. Saleeby, Y. Zhu, T. Romanazzi, P. Ulery-Reynolds, I. Bahar, A. M. Carter, H. J. G. Matthies and A. Galli, *Sci. Adv.*, 2023, **9**, eadd8417.
17 X. Li, S. Majdi, J. Dunevall, H. Fathali and A. G. Ewing, *Angew. Chem., Int. Ed.*, 2015, **54**, 11978–11982.
18 X. K. Yang, F. L. Zhang, W. T. Wu, Y. Tang, J. Yan, Y. L. Liu, C. Amatore and W. H. Huang, *Angew. Chem., Int. Ed.*, 2021, **60**, 15803–15808.
19 C. Gu, A. Larsson and A. G. Ewing, *Proc. Natl. Acad. Sci. U. S. A.*, 2019, **116**, 21409–21415.
20 X. He and A. G. Ewing, *Chem. Sci.*, 2022, **13**, 1815–1822.
21 Y. Wang, C. Gu and A. G. Ewing, *Angew. Chem., Int. Ed.*, 2022, **61**, e202200716.
22 Y. T. Li, S. H. Zhang, L. Wang, R. R. Xiao, W. Liu, X. W. Zhang, Z. Zhou, C. Amatore and W. H. Huang, *Angew. Chem., Int. Ed.*, 2014, **53**, 12456–12460.
23 Y. T. Li, S. H. Zhang, X. Y. Wang, X. W. Zhang, A. I. Oleinick, I. Svir, C. Amatore and W. H. Huang, *Angew. Chem., Int. Ed.*, 2015, **54**, 9313–9318.
24 Y. Tang, X. K. Yang, X. W. Zhang, W. T. Wu, F. L. Zhang, H. Jiang, Y. L. Liu, C. Amatore and W. H. Huang, *Chem. Sci.*, 2020, **11**, 778–785.
25 N. X. Tritsch and B. L. Sabatini, *Neuron*, 2012, **76**, 33–50.
26 M. B. Hoppa, G. Gouzer, M. Armbruster and T. A. Ryan, *Neuron*, 2014, **84**, 778–789.

27 G. F. Kusick, M. Chin, S. Raychaudhuri, K. Lippmann, K. P. Adula, E. J. Hujber, T. Vu, M. W. Davis, E. M. Jorgensen and S. Watanabe, *Nat. Neurosci.*, 2020, **23**, 1329–1338.
28 M. Borisovska, A. L. Bensen, G. Chong and G. L. Westbrook, *J. Neurosci.*, 2013, **33**, 1790–1796.
29 J. J. Lefkowitz, V. Decrescenzo, K. Duan, K. D. Bellve, K. E. Fogarty, J. V. Walsh and R. Zhuge, *J. Physiol.*, 2014, **592**, 4639–4655.
30 Y. Park and K. Kim, *Cell. Signalling*, 2009, **21**, 1465–1470.
31 G. Thiel, *Brain Pathol.*, 1993, **3**, 87–95.
32 J. Alder, H. Kanki, F. Valtorta, P. Greengard and M. Poo, *J. Neurosci.*, 1995, **15**, 511–519.
33 J. H. Koenig and K. Ikeda, *J. Neurophysiol.*, 1999, **81**, 1495–1505.
34 V. I. Torres and N. C. Inestrosa, *Mol. Neurobiol.*, 2018, **55**, 4513–4528.
35 C. M. Bittins, T. W. Eichler and H. Gerdes, *Cell. Mol. Neurobiol.*, 2009, **29**, 597–608.
36 A. N. van den Pol, *Neuron*, 2012, **76**, 98–115.
37 A. P. Bolshakov and A. V. Rozov, *J. Neurochem.*, 2014, **8**, 238–246.
38 S. Miyamoto, *Biochim. Biophys. Acta, Gen. Subj.*, 1995, **1244**, 85–91.
39 T. Hökfelt, D. Millhorn, K. Seroogy, Y. Tsuruo, S. Ceccatelli, B. Lindh, B. Meister, T. Melander, M. Schalling, T. Bartfai and L. Terenius, *Experientia*, 1987, **43**, 768–780.
40 A. Merighi, C. Salio, F. Ferrini and L. Lossi, *J. Chem. Neuroanat.*, 2011, **42**, 276–287.
41 C. E. Vaaga, B. Maria and W. Gary L, *Curr. Opin. Neurobiol.*, 2014, **29**, 25–32.
42 W. J. Jockusch, D. Speidel, A. Sigler, J. B. Sørensen, F. Varoqueaux, J. Rhee and N. Brose, *Cell*, 2007, **131**, 796–808.